TÜBİTAK

Turkish Journal of Medical Sciences

http://journals.tubitak.gov.tr/medical/

Research Article

Turk J Med Sci
(2023) 53: 1807-1816
© TÜBİTAK
doi:10.55730/1300-0144.5751

# Assessment of changes in macular structural retinal layers in patients with pathological myopia

**Mehmet ÇITIRIK[1,*], Kamil YAVUZER[2], Fatma BAĞCI[1]**

[1]Department of Ophthalmology, University of Health Sciences, Ankara Etlik City Hospital, Ankara, Turkiye
[2]Department of Ophthalmology, Dünya Göz Hospital, Gaziantep, Turkiye

**Received:** 09.05.2023 • **Accepted/Published Online:** 25.10.2023 • **Final Version:** 12.12.2023

**Background/aim:** This study aimed to examine changes in the thickness of individual macular retinal layers in eyes with pathological myopia (PM) and to compare the thickness of each retinal layer between the PM and control groups to gain insights into retinal perfusion.

**Materials and methods:** The study included 51 eyes in the PM group and 51 eyes in the control group. Optical coherence tomography (OCT) was used to measure the thickness of each retinal layer in the central fovea, parafoveal, and perifoveal regions. Optical coherence tomography angiography (OCT-A) was used to evaluate the retinal capillary density.

**Results:** In the PM group, the retinal nerve fiber layer (RNFL), ganglion cell layer (GCL), inner plexiform layer (IPL), and inner nuclear layer (INL) were thicker than in the control group ($p = 0.004$, $p = 0.027$, $p = 0.020$, and $p < 0.001$, respectively), whereas the outer nuclear layer (ONL) and photoreceptor layer (PRL) were thinner ($p = 0.001$ and $p = 0.003$, respectively). In other regions, the RNFL was thicker in the myopic group, whereas the GCL, IPL, INL, and ONL were thinner. OCT-A did not reveal any significant difference between the groups in terms of radial capillary plexus density ($p = 0.381$); however, the densities of the other plexuses were lower in the PM group.

**Conclusions:** The results showed alterations in the thickness of retinal layers and capillary plexus density in PM. Thus, assessment of the thickness of individual retinal layers may serve as an indicator of vascular diseases that affect the circulation of the retina and choroid.

**Key words:** Choroid, optical coherence tomography, optical coherence tomography angiography, pathological myopia, retinal segmentation analysis

## 1. Introduction

Globally, myopia is a significant public health issue [1], with high myopia (HM) traditionally defined as a refractive error with a spherical equivalent exceeding –6.0 diopters (D) and/or an axial length greater than 26.5 mm [2]. HM is the leading cause of uncorrected visual acuity loss and the primary cause of low vision and blindness worldwide [3–5].

Pathological myopia (PM) differs from other types of myopia in that it causes the loss of best-corrected visual acuity (BCVA) [6]. It was first defined as the presence of structural changes that cause vision loss [7], and is now commonly defined as myopia with posterior segment complications owing to progressive and excessive elongation of the eyeball. Axial elongation is believed to play a key role in degenerative changes [8], and the prevalence of PM has increased exponentially [9].

Spectral-domain optical coherence tomography (SD-OCT) devices offer non-invasive cross-sectional imaging of the retina. Segmentation analysis using the latest SD-OCT software enables more straightforward and accurate automatic differentiation of each retinal layer, allowing for separate measurements of the thickness of each layer [10]. With this technological advancement, scientists have been able to assess retinal layer thickness in PM [11–13].

The retinal structures are supplied by blood vessels that originate from the choroid and retina. There are 3 retinal capillary plexuses, namely the radial peripapillary capillary plexus (RPCP), the superficial capillary plexus (SCP), and the deep capillary plexus (DCP), in addition to the choriocapillaris [14]. Optical coherence tomography angiography (OCT-A) is a novel noninvasive imaging technique that enables the visualization of retinal vessels and provides quantitative data on the density of these vascular plexuses.

The main objective of our research was to examine and compare the thicknesses of the retinal layers in the macular areas of eyes with PM and eyes in a control group. Another goal was to gain a better understanding of retinal

* Correspondence: mcitirik@hotmail.com

perfusion by analyzing the variations in layer thickness between the myopic and control groups.

## 2. Materials and methods

This retrospective study was approved by the local ethics committee and adhered to the principles of the Declaration of Helsinki. The study included 2 subgroups: the myopic group with a spherical equivalent of –6.00 to –10.00 D and an axial length between 26.5 and 28.5 mm, and the control group with a spherical equivalent of –1.00 D to +1.00 D and an axial length between 22.00 mm and 24.00 mm. The study employed the classification of the META-analysis for PM study group [15] and included cases with PM but with an unaffected macular area and no additional chorioretinal degenerative findings, excluding the macular region.

The study excluded patients with systemic diseases such as diabetes mellitus or hypertension; ocular diseases that require chronic medication use such as uveitis, glaucoma, and dry eye; a history of intraocular surgery or trauma; and additional findings affecting the macular region such as myopic retinoschisis, drusen, pigment epithelial detachment, vitreomacular traction, epiretinal membrane, or choroidal neovascularization. The study included 51 eyes of 34 patients in the myopia group and 51 eyes of 26 patients in the control group. Only one patient in the control group, who had a cataract in one eye, did not have both eyes included in the study. Patients with additional pathologies affecting the macular region of the fellow eye were not included in the myopic group. Additionally, cases with artifacts in the measurements and unqualified retinal segmentation analysis were excluded from the study.

Prior to the study, all patients underwent a comprehensive eye examination that included measuring refractive errors with an autorefractometer (Ark-la Auto Ref/Keratometer, Nidek Co. Ltd., Japan), intraocular pressure with a fully automatic noncontact tonometer (Topcon Computerized Tonometer, Topcon Corporation, Japan), and best-corrected visual acuity using a Snellen chart, which was converted to the logarithm of the minimum angle of resolution (LogMAR). Axial lengths were measured using an optical biometry device (Lenstar LS 900, Haag-Streit, Switzerland). Fundoscopic examination was performed after the slit-lamp examination, and fundus photographs were taken in seven regions using a digital retinal camera system (Zeiss Visucam NM Pro Fundus Camera, ZEISS, Jena, Germany).

An AngioVue OCTA instrument (RTVue XR Avanti, version 2017.1.0.151; Optovue, Inc., Fremont, CA, USA) was used to obtain the densities of the RPCP, SCP, and DCP. However, low-quality images with a signal strength below 7 or the presence of blinking, poor fixation, or segmentation errors that caused motion or double artifacts were excluded from the study.

An SD-OCT device (HRA2-Heidelberg Retina Angiography-Optical Coherence Tomography, Heidelberg Engineering, Heidelberg, Germany) was used to measure the total retinal thickness (TRT) and retinal layer thickness in the macular region. Thickness measurements were performed without correction formulas because of the automatic correction feature of the device between +12.0 D and –24.0 D. The SD-OCT scans usually covered 6 × 6 mm square sections centered on the fovea, with 2 data points obtained: numerical data showing the average retinal thickness in the area of interest and color-coded images for comparison with normative data. The Early Treatment Diabetic Retinopathy Study (ETDRS) grid was used to identify 9 regions of the retinal map on SD-OCT. The foveal area was defined as a central circle with a diameter of 1 mm centered on the foveola, the parafoveal region was defined as the area surrounding the foveal area with a diameter of 2 mm, and the perifoveal region was defined as the area surrounding the parafoveal region with a diameter of 3 mm (Figure 1a). The automatic segmentation of macular retinal layers (Figure 1b) included the retinal nerve fiber layer (RNFL), ganglion cell layer (GCL), inner plexiform layer (IPL), inner nuclear layer (INL), outer plexiform layer (OPL), outer nuclear layer (ONL), photoreceptor layer (PRL), and retinal pigment epithelium (RPE). The sum of the thicknesses of the RNFL + GCL + IPL + INL was defined as the inner retinal thickness (IRT), while the sum of the thicknesses of the OPL + ONL + PRL was defined as the outer retinal thickness (ORT) (Figure 1c).

Statistical analyses were performed using STATA 15 software. According to the Bonferroni procedure for multiple comparisons, a 2-sample t-test was used to compare the mean differences in retinal layer thickness between the myopic and control groups. Statistical significance was set at $p < 0.05$.

## 3. Results

Table 1 provides a summary of the demographic data and statistical analysis comparing the PM and control groups, which showed no significant differences in age, sex, or intraocular pressure ($p = 0.087$, $p = 1.000$, and $p = 0.960$, respectively). However, patients with PM had higher refractive errors, worse BCVA, and longer axial lengths than those in the control group ($p < 0.001$, $p < 0.001$, and $p = 0.009$, respectively).

The central foveal region (1 mm) in the PM group exhibited a significantly thicker RNFL, GCL, IPL, INL, and IRT ($p < 0.05$). Although the TRT and OPL were thicker than those in the control group, this difference was not statistically significant ($p > 0.05$). Furthermore, the ONL, PRL, and ORT were significantly thinner in the PM group ($p < 0.05$), and while the RPE was thinner in the PM group, the difference was not statistically significant ($p = 0.115$).

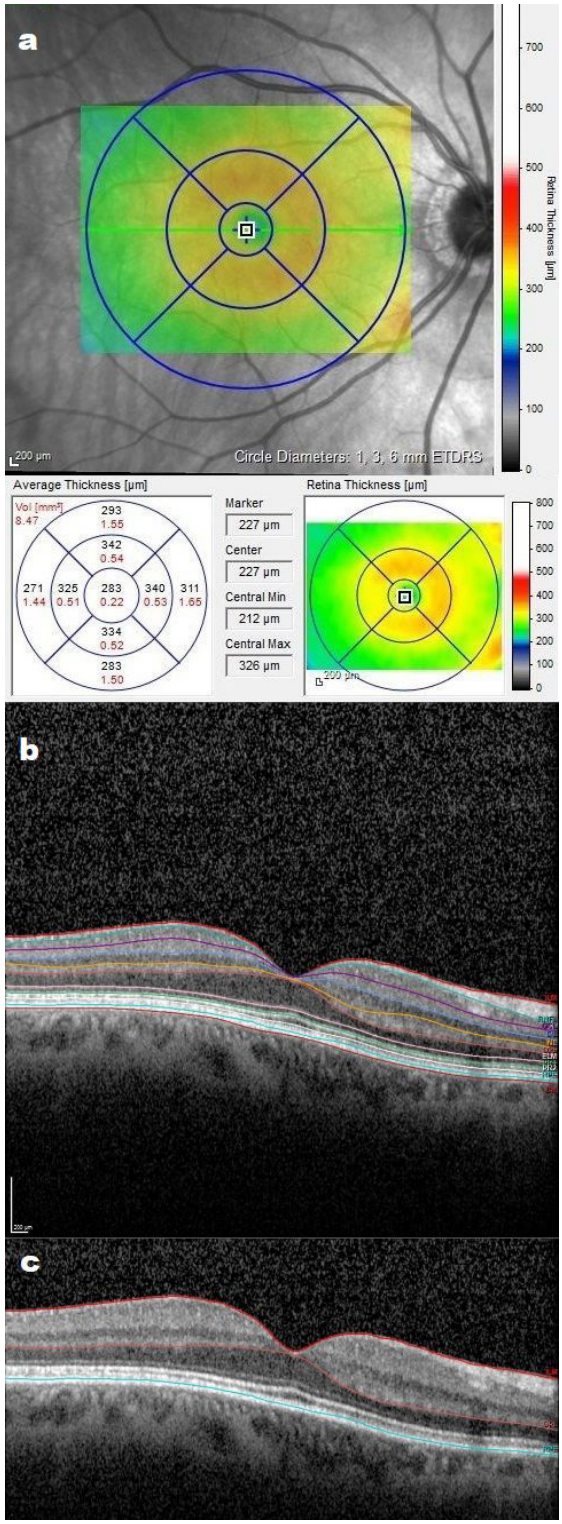


**Figure 1.** (a) Nine regions of the macular retina map defined by the ETDRS grid. (b) OCT image showing all retinal layers in a myopic case. (c) Appearance of the inner and outer retinal layers. The part from the inner retina is from the ILM to the INL–OPL border. The outer retina is from the INL–OPL border to the RPE.

**Table 1.** Characteristics and demographic features of the groups.

| Parameters | PM group | Control group | p |
|---|---|---|---|
| Age (years) | 58.2 ± 10.5 | 53.9 ± 14.0 | 0.087 |
| Sex, n (male/female) | 27/24 | 27/24 | 1.000 |
| Spherical equivalent (diopter) | -8.76 ± 1.82 | -0.25 ± 0.48 | **<0.001** |
| BCVA (logMAR) | 0.08 ± 0.75 | 0.01 ± 1.29 | **<0.001** |
| Intraocular pressure (mmHg) | 14.10 ± 3.4 | 12.65 ± 3.4 | 0.960 |
| Axial length (mm) | 27.64 ± 0.77 | 22.96 ± 0.57 | **0.009** |

BCVA = best-corrected visual acuity; logMAR = logarithm of the minimum angle of resolution. Bold text indicates statistical significance.

Tables 2 and 3 display the measured thicknesses of each retinal layer obtained through the retinal segmentation analysis.

Retinal layer thickness was analyzed in 4 regions surrounding the central 1 mm circle in the parafoveal region, including the superior, inferior, temporal, and nasal regions. The PM group had a significantly thicker RNFL in the superior parafoveal region ($p = 0.001$), but thinner TRT, GCL, IPL, INL, ONL, IRT, and ORT ($p < 0.05$). The PM group also had a thinner OPL, PRL, and RPE, although this difference was not statistically significant ($p > 0.05$). In the parafovea inferior region, the OPL was significantly thicker in the PM group ($p = 0.012$), and while the RNFL was also thicker, the difference was not statistically significant ($p = 0.186$). The thicknesses of the TRT, GCL, IPL, INL, ONL, IRT, and ORT were significantly lower in the PM group than in the control group ($p < 0.05$), whereas there was no significant difference in the thickness of the PRL and RPE between the 2 groups ($p = 0.473$ and $p = 0.625$, respectively). In the parafoveal nasal region, the myopic group showed significant thickening of the RNFL and OPL ($p = 0.001$ for both), and the INL was thicker, but not significantly ($p = 0.782$). In contrast, the TRT, GCL, IPL, ONL, and ORT were significantly thinner in the PM group ($p < 0.05$), and the RPE, PRL, and IR were thinner but not statistically significant ($p > 0.05$). In the parafoveal temporal region, the PM group showed significant RNFL thickening ($p = 0.001$), whereas TRT, GCL, IPL, INL, ONL, IRT, and ORT were significantly thinner ($p < 0.05$). The OPL, PRL, and RPE were also thinner, but not significantly ($p > 0.05$).

Four perifoveal regions were analyzed. In the perifoveal superior region, the RNFL and RPE were thicker in the PM group than in the control group; however, the difference was not statistically significant ($p = 0.249$ and $p = 0.409$, respectively). TRT, GCL, IPL, INL, ONL, IRT, and ORT were significantly thinner in the PM group ($p < 0.05$); INL and PRL were also thinner, but the difference was not statistically significant ($p > 0.05$). In the perifoveal inferior region, the INL, OPL, PRL, and RPE were thicker in the PM group, but the difference was not statistically significant ($p > 0.05$). The TRT, GCL, IPL, INL, ONL, IRT, and ORT were significantly thinner in the PM group ($p < 0.05$); the RNFL and IPL were also thinner, but the difference was not statistically significant ($p = 0.256$ and $p = 0.885$, respectively).

The PM group showed a significant increase in RNFL thickness ($p = 0.013$) in the perifoveal nasal region; while the thicknesses of the OPL, PRL, and RPE were also higher, this difference was not statistically significant ($p > 0.05$). Additionally, the TRT, GCL, ONL, and ORT were significantly thinner in the PM group ($p < 0.05$); the IPL, INL, and IRT were thinner but not significantly ($p > 0.05$). The PM group showed a significant increase in RNFL thickness in the perifoveal temporal region ($p < 0.001$) as well as a non-significant increase in PRL and RPE thickness ($p > 0.05$). Meanwhile, TRT, IPL, GCL, INL, OPL, ONL, IRT, and ORT were significantly thinner in the PM group ($p < 0.05$).

The PM group had a RPCP density of 46.89 ± 2.42%, which was not significantly different from the RPCP density of 49.44 ± 2.83% in the control group ($p = 0.381$). However, the PM group had lower densities in both SCP and DCP, with SCP density at 41.18 ± 0.68% and DCP density at 42.90 ± 1.36%, compared to the control group's SCP density of 48.03 ± 1.33% and DCP density of 49.33 ± 2.51% ($p = 0.003$ and $p = 0.040$, respectively).

## 4. Discussion

Retinal diseases often involve vascular pathologies due to the rich vascular supply of the retina provided by the 3 plexuses and the choroid. The RNFL is supplied by the RPCP, the GCL and IPL are fed by the SCP, and the INL and OPL are supplied by the DCP. The choroid, a tissue with a rich vascular supply in the body, supplies the outer retinal layers through diffusion [16,17]. Measuring the

**Table 2.** Thicknesses of RNFL, GCL, IPL, INL, OPL, ONL, PRL, and RPE in both groups.

| Layer | Retinal region | PM group, mean values ± SD (µm) | Control group, mean values ± SD (µm) | p |
|---|---|---|---|---|
| RNFL | Central | 16.5 ± 5.7 | 13.7 ± 3.5 | **0.004** |
| | PaFoSu | 31.3 ± 7.0 | 25.4 ± 3.5 | **<0.001** |
| | PeFoSu | 40.3 ± 8.2 | 38.5 ± 7.0 | 0.249 |
| | PaFoNa | 27.8 ± 6.0 | 23.3 ± 6.0 | **0.001** |
| | PeFoNa | 57.0 ± 13.9 | 50.9 ± 9.7 | **0.013** |
| | PaFoTe | 21.7 ± 6.4 | 18.3 ± 2.6 | **0.001** |
| | PeFoTe | 23.0 ± 3.7 | 19.5 ± 2.0 | **<0.001** |
| | PaFoIn | 28.2 ± 6.3 | 26.8 ± 4.5 | 0.186 |
| | PeFoIn | 37.7 ± 8.8 | 39.4 ± 6.4 | 0.256 |
| GCL | Central | 22.4 ± 10.0 | 18.3 ± 7.9 | **0.027** |
| | PaFoSu | 45.2 ± 9.1 | 52.7 ± 5.6 | **<0.001** |
| | PeFoSu | 29.8 ± 5.7 | 36.4 ± 4.4 | **<0.001** |
| | PaFoNa | 44.7 ± 10.0 | 51.9 ± 5.3 | **<0.001** |
| | PeFoNa | 31.4 ± 5.6 | 38.5 ± 3.7 | **<0.001** |
| | PaFoTe | 41.2 ± 8.6 | 47.8 ± 4.9 | **<0.001** |
| | PeFoTe | 29.1 ± 5.3 | 37.2 ± 4.6 | **<0.001** |
| | PaFoIn | 41.5 ± 10.5 | 52.0 ± 6.4 | **<0.001** |
| | PeFoIn | 29.9 ± 7.1 | 35.5 ± 4.6 | **<0.001** |
| IPL | Central | 25.8 ± 6.5 | 23.0 ± 5.2 | **0.020** |
| | PaFoSu | 37.3 ± 6.0 | 41.0 ± 4.1 | **0.001** |
| | PeFoSu | 26.3 ± 4.0 | 29.1 ± 2.8 | **<0.001** |
| | PaFoNa | 39.4 ± 6.1 | 42.5 ± 4.1 | **0.003** |
| | PeFoNa | 28.5 ± 4.9 | 29.7 ± 2.8 | 0.132 |
| | PaFoTe | 38.5 ± 5.5 | 41.4 ± 4.4 | **0.005** |
| | PeFoTe | 29.2 ± 3.6 | 33.1 ± 3.0 | **<0.001** |
| | PaFoIn | 36.7 ± 5.7 | 41.0 ± 4.0 | **<0.001** |
| | PeFoIn | 27.0 ± 4.4 | 28.5 ± 3.3 | 0.065 |
| INL | Central | 29.1 ± 10.1 | 22.0 ± 7.3 | **<0.001** |
| | PaFoSu | 37.5 ± 4.7 | 42.6 ± 3.8 | **<0.001** |
| | PeFoSu | 31.9 ± 5.7 | 33.3 ± 2.8 | 0.152 |
| | PaFoNa | 42.0 ± 6.9 | 41.7 ± 4.3 | 0.782 |
| | PeFoNa | 34.0 ± 5.8 | 34.7 ± 2.7 | 0.451 |
| | PaFoTe | 35.8 ± 3.9 | 38.1 ± 3.4 | **0.002** |
| | PeFoTe | 30.0 ± 3.5 | 33.9 ± 2.7 | **<0.001** |
| | PaFoIn | 38.9 ± 7.3 | 41.5 ± 3.7 | **0.028** |
| | PeFoIn | 33.9 ± 6.6 | 32.8 ± 3.5 | 0.297 |

**Table 1.** (Continued).

| | | | | |
|---|---|---|---|---|
| **OPL** | Central | 31.3 ± 10.7 | 27.1 ± 11.2 | 0.054 |
| | PaFoSu | 33.5 ± 8.0 | 35.2 ± 8.1 | 0.279 |
| | PeFoSu | 27.1 ± 3.1 | 28.4 ± 3.2 | **0.041** |
| | PaFoNa | 42.6 ± 14.2 | 34.4 ± 8.0 | **0.001** |
| | PeFoNa | 30.7 ± 4.5 | 29.6 ± 3.1 | 0.139 |
| | PaFoTe | 30.0 ± 6.3 | 31.0 ± 5.1 | 0.353 |
| | PeFoTe | 26.4 ± 3.0 | 27.5 ± 2.2 | **0.028** |
| | PaFoIn | 37.8 ± 7.2 | 33.9 ± 8.1 | **0.012** |
| | PeFoIn | 29.5 ± 4.3 | 28.4 ± 5.2 | 0.275 |
| **ONL** | Central | 77.6 ± 19.8 | 90.0 ± 15.2 | **0.001** |
| | PaFoSu | 62.0 ± 11.5 | 68.4 ± 14.3 | **0.015** |
| | PeFoSu | 56.0 ± 9.6 | 60.2 ± 8.6 | **0.024** |
| | PaFoNa | 56.3 ± 13.3 | 71.9 ± 13.0 | **<0.001** |
| | PeFoNa | 47.2 ± 8.6 | 56.1 ± 7.8 | **<0.001** |
| | PaFoTe | 67.2 ± 12.3 | 74.4 ± 8.9 | **0.001** |
| | PeFoTe | 52.2 ± 8.4 | 59.6 ± 6.9 | **<0.001** |
| | PaFoIn | 57.8 ± 17.7 | 67.7 ± 10.7 | **0.001** |
| | PeFoIn | 45.3 ± 9.3 | 53.7 ± 7.4 | **<0.001** |
| **PRL** | Central | 83.7 ± 7.4 | 87.4 ± 4.1 | **0.003** |
| | PaFoSu | 79.3 ± 6.2 | 81 ± 3.3 | 0.088 |
| | PeFoSu | 78.5 ± 6.9 | 79.1 ± 2.8 | 0.574 |
| | PaFoNa | 79.8 ± 7.8 | 81.8 ± 3.1 | 0.089 |
| | PeFoNa | 79.1 ± 6.5 | 78.5 ± 2.4 | 0.556 |
| | PaFoTe | 79.5 ± 5.5 | 81.1 ± 2.9 | 0.063 |
| | PeFoTe | 78.2 ± 6.3 | 78 ± 2.9 | 0.809 |
| | PaFoIn | 78.8 ± 6.7 | 79.6 ± 3.9 | 0.473 |
| | PeFoIn | 76.9 ± 5.7 | 76.7 ± 2.2 | 0.885 |
| **RPE** | Central | 15.4 ± 4.8 | 16.6 ± 1.7 | 0.115 |
| | PaFoSu | 14.1 ± 3.6 | 15.0 ± 1.8 | 0.102 |
| | PeFoSu | 14.3 ± 6.4 | 13.5 ± 1.2 | 0.409 |
| | PaFoNa | 14.1 ± 4.9 | 15.0 ± 1.8 | 0.190 |
| | PeFoNa | 14.4 ± 4.5 | 13.3 ± 1.3 | 0.104 |
| | PaFoTe | 14.0 ± 2.7 | 14.2 ± 1.4 | 0.648 |
| | PeFoTe | 14.2 ± 5.3 | 12.9 ± 1.4 | 0.097 |
| | PaFoIn | 13.9 ± 3.9 | 14.4 ± 1.6 | 0.424 |
| | PeFoIn | 13.2 ± 3.2 | 13.0 ± 1.1 | 0.625 |

SD = standard deviation; RNFL = retinal nerve fiber layer; GCL = ganglion cell layer; IPL = inner plexiform layer; INL = inner nuclear layer; OPL = outer plexiform layer; ONL = outer nuclear layer; PRL = photoreceptor layer; RPE = retinal pigment epithelium; PaFoSu = parafovea superior; PeFoSu = perifovea superior; PaFoNa = parafovea nasal; PeFoNa = perifovea nasal; PaFoTe = parafovea temporal; PeFoTe = perifovea temporal; PaFoIn = parafovea inferior; PeFoIn = perifovea inferior. Bold text indicates statistical significance.

**Table 3.** TRK, IRT, and ORT thickness values in both groups.

| Layer | Retinal region | PM group, mean values ± SD (μm) | Control group, mean values ± SD (μm) | p |
|---|---|---|---|---|
| **TRT** | Central | 284.9 ± 29.6 | 278.6 ± 25.8 | 0.253 |
| | PaFoSu | 325.0 ± 25.5 | 344.6 ± 21.4 | <0.001 |
| | PeFoSu | 287.5 ± 22.1 | 304.5 ± 15.7 | **<0.001** |
| | PaFoNa | 330.0 ± 25.6 | 347.5 ± 15.6 | **<0.001** |
| | PeFoNa | 304.0 ± 26.9 | 318.0 ± 13.7 | **0.002** |
| | PaFoTe | 313.2 ± 23.7 | 332.3 ± 13.5 | <0.001 |
| | PeFoTe | 267.3 ± 17.5 | 289.0 ± 11.8 | **<0.001** |
| | PaFoIn | 318.8 ± 26.9 | 342.5 ± 15.1 | **<0.001** |
| | PeFoIn | 278.7 ± 23.3 | 295.0 ± 16.6 | **<0.001** |
| **IRT** | Central | 93.8 ± 27.5 | 77.1 ± 22.6 | 0.001 |
| | PaFoSu | 151.2 ± 19.2 | 161.7 ± 12.2 | **0.002** |
| | PeFoSu | 128.3 ± 15.1 | 137.3 ± 12.3 | **0.002** |
| | PaFoNa | 153.9 ± 19.0 | 159.4 ± 11.5 | 0.081 |
| | PeFoNa | 150.8 ± 18.5 | 153.7 ± 10.9 | 0.335 |
| | PaFoTe | 137.2 ± 15.9 | 145.6 ± 11.7 | **0.003** |
| | PeFoTe | 111.3 ± 12.0 | 123.8 ± 9.2 | **<0.001** |
| | PaFoIn | 145.5 ± 22.9 | 161.3 ± 15.0 | **<0.001** |
| | PeFoIn | 128.5 ± 16.4 | 136.2 ± 10.4 | **0.006** |
| **ORT** | Central | 192.6 ± 22.2 | 204.5 ± 12.4 | **0.001** |
| | PaFoSu | 175.2 ± 14.4 | 184.6 ± 10.9 | **0.001** |
| | PeFoSu | 161.8 ± 14.4 | 167.7 ± 9.0 | **0.017** |
| | PaFoNa | 178.7 ± 17.5 | 188.1 ± 12.5 | 0.003 |
| | PeFoNa | 157.3 ± 13.6 | 164.2 ± 8.5 | **0.003** |
| | PaFoTe | 176.6 ± 15.1 | 186.6 ± 10.6 | **<0.001** |
| | PeFoTe | 156.8 ± 12.3 | 165.2 ± 9.0 | **<0.001** |
| | PaFoIn | 174.5 ± 20.4 | 181.2 ± 12.3 | **0.047** |
| | PeFoIn | 151.7 ± 14.2 | 158.8 ± 9.7 | **0.004** |

SD = standard deviation; TRT = total retinal thickness; IRT = inner retinal thickness; ORT = outer retinal thickness; PaFoSu = parafovea superior; PeFoSu = perifovea superior; PaFoNa = parafovea nasal; PeFoNa = perifovea nasal; PaFoTe = parafovea temporal; PeFoTe = perifovea temporal; PaFoIn = parafovea inferior; PeFoIn = perifovea inferior. Bold text indicates statistical significance.

thickness of the intraretinal layers can provide important information about retinal perfusion in the diagnosis and progression of retinal diseases. Therefore, our study aimed to enhance the understanding of retinal perfusion by separately measuring the macular thickness of the intraretinal layers.

We found a decrease in the thickness of the inner retinal layers and an increase in RNFL thickness in the PM group compared with the control group. This finding is consistent with a previous study by Kim et al. [11], who reported thicker RNFL and retinal layer in highly myopic eyes than in nonmyopic eyes. Another study by Liu et al. [13] reported a significant increase in RNFL thickness in highly myopic eyes. However, unlike the findings of Kim et al., the thicknesses of the GCL, IPL, and INL in their myopic group were similar to those found in the current study. In contrast, our study showed that the density of both SCP and DCP decreased in the PM group compared to that in the control group, while RPCP density did not show a significant decrease. The lack of a decrease in RNFL thickness could be attributed to the presence of large retinal vessels located in close proximity to the RPCP. As per previous research [12,14], RPCP density is considered less responsive to alterations during pathological progression linked with high myopia. In contrast to the other retinal layers, the thickness of the OPL did not significantly decrease in the PM group in our study. This can be explained by the fact that the OPL has a unique vascular supply, with the inner part being fed by the DCP and the outer part by the choriocapillaris [12,17,18]. Therefore, the dual nutrition system may have contributed to the minimal decrease in OPL thickness observed in our study.

We observed that the most notable reduction in the retinal layer thickness occurred in the ONL. Because the ONL consists of photoreceptor nuclei, it requires a rich vascular supply to maintain sufficient oxygenation. Therefore, a decrease in ONL thickness may indicate photoreceptor damage [19]. Previous studies have reported that diseases caused by choroidal ischemia are associated with thinner ONL, suggesting that choroidal ischemia may contribute to such damage [20]. We suggest that the decrease in choroidal thickness in myopic eyes affects external retinal perfusion because the choroid does not have a rich vascular network that feeds the retinal tissue. However, Ye et al. [12] reported that despite the reduction in choroidal thickness, oxygen diffusion from the choroid was sufficient to meet the demands of the outer retinal sublayers. They also found that this diffusion partially prevented visual impairment, indicating that visual function remained normal and stable in high myopia. This conclusion is similar to our findings, as we observed a decrease in ONL thickness, whereas PRL and RPE remained unchanged.

A histological study of enucleated eyes and an in vivo study of choroidal and retinal thicknesses revealed that myopia was associated with reductions in both choroidal and retinal thickness [21,22]. Abbott et al. [23] also reported retinal thinning in both in vivo OCT images and in vitro histological analysis of a mammalian animal model of myopia compared to control eyes. Consistent with previous studies [24,25], we observed thinning in both the IRL and ORL, except for in the central 1 mm region, in our study's PM group. The reduction in peripheral retinal thickness observed in myopic eyes may be due to the absence of large vessels and optic fibers in the peripheral retina, making it less resistant to pulling and stretching. This thinning in the periphery may compensate for the tensile force on the entire retina and maintain the thickness of the central retina [26,27]. Therefore, as axial length increases in myopia, peripheral retinal thinning occurs, while the central macular area remains relatively protected. This finding is consistent with the observations of the present study.

In our study, we found that both IRL and ORL were affected by PM. This suggests that various conditions observed in pathological myopic eyes, including macular atrophy, peripapillary atrophy, peripheral chorioretinal atrophic areas, and lattice-like lesions, may be attributed to this insufficient vascular environment. Li et al. [28] observed a significant reduction in the density of both the superficial and deep retinal vascular plexuses in eyes with PM, as measured by OCTA, compared to the control group. They attributed this decrease to the elongation of the eye due to the progression of myopia. In a prior study, Mo et al. [29] used OCTA to examine PM and reported no notable variance in RPCP flow density between the PM and control groups. Wang et al. [30] evaluated the retinal vascular density in youth myopia without maculopathy with OCTA. They found that the retinal vascular density decreased in the high myopia group. They emphasized that the microvascular network inside the disc may have a compensatory action in the hypoxic setting of high myopia. Ye et al. [31] analyzed the radial peripapillary capillary density and the peripapillary retinal nerve fiber layer thickness in pathological myopia. They concluded that peripapillary alterations, both decreasing radial peripapillary capillary density and peripapillary retinal nerve fiber layer thickness, occurred in PM compared to controls. The present study revealed a significant decrease in the density of both superficial and deep vascular plexuses, while RPCP density was only moderately reduced and was not significantly different from that of the control group. Assessing the density of retinal vascular structures using OCT-A is a notable strength of our study, as it enables the evaluation of the vascular status of each individual retinal layer.

In conclusion, our findings indicate that PM results in a decrease in total retinal thickness, primarily in the outer retina of the fovea and both inner and outer retinal layers in the extrafoveal regions. While thinning occurs in the inner retinal layers, RNFL thickness does not decrease significantly, indicating that RPCP is less affected than other retinal vascular structures in high myopia. We posit that the demonstration of vascular insufficiency in certain sublayers of the retina in PM may serve as evidence for vascular diseases affecting retinal and choroidal circulation.

## 5. Disclosures

This study was presented at the EURETINA 2021 virtual meeting, September 9–12, 2021. This paper has not been published nor submitted simultaneously for publication elsewhere.

### Conflict of interest statement

The authors declare that they have no conflicts of interest. They also have no proprietary or financial interest in the products mentioned in this study.

### Informed consent and human and animal rights statement

Informed consent was obtained from all individuals included in this study.

### Ethics committee approval

The research related to human use complied with all relevant national regulations and institutional policies, followed the tenets of the Helsinki Declaration, and was

approved by the Ethics Committee of the Van Training and Research Hospital, Van, Turkey (No:2020/15).

**Author contributions**

Conception: KY, FB, MC; design: KY, FB, MC; supervision: MC; resources: MC; materials: KY, FB; data collection and/or processing: KY, FB; analysis and/or interpretation: KY, MC; literature search: KY, MC; writing: KY, MC; critical reviews; MC.

**Peer review**

Externally peer reviewed.

**Sources of funding**

This research did not receive any specific grants from funding agencies in the public, commercial, or not-for-profit sectors.

**References**

1. Naidoo KS, Fricke TR, Frick KD, Jong M, Naduvilath TJ et al. Potential lost productivity resulting from the global burden of myopia: Systematic review, meta-analysis, and modeling. Ophthalmology 2019; 126 (3): 338-346. https://doi.org/10.1016/j.ophtha.2018.10.029
2. Ludwig CA, Shields RA, Chen TA, Powers MA, Wilkin Parke III D et al. A novel classification of high myopia into anterior and posterior pathologic subtypes. Graefe's Archive for Clinical and Experimental Ophthalmology 2018; 256 (10): 1847-1856. https://doi.org/10.1007/s00417-018-4071-0
3. Sawada A, Tomidokoro A, Araie M, Iwase A, Yamamoto T. Refractive errors in an elderly Japanese population: The Tajimi study. Ophthalmology 2008; 115 (2): 363-370.e3. https://doi.org/10.1016/j.ophtha.2007.03.075
4. Xu L, Li J, Cui T, Hu A, Fan G et al. Refractive error in urban and rural adult Chinese in Beijing. Ophthalmology 2005; 112 (10): 1676-1683. https://doi.org/10.1016/j.ophtha.2005.05.015
5. Cotter SA, Varma R, Ying-Lai M, Azen SP, Klein R. Causes of low vision and blindness in adult Latinos: The Los Angeles Latino eye study. Ophthalmology 2006; 113 (9): 1574-1582. https://doi.org/10.1016/j.ophtha.2006.05.002
6. Ohno-Matsui K. Pathologic Myopia. Asia-Pacific Journal of Ophthalmology 2016; 5 (6): 415-423. https://doi.org/10.1097/APO.0000000000000230
7. Morgan IG, Ohno-Matsui K, Saw SM. Myopia. The Lancet 2012; 379 (9827): 1739-1748. https://doi.org/10.1016/S0140-6736(12)60272-4
8. Wang NK, Wu YM, Wang JP, Liu L, Yeung L et al. Clinical characteristics of posterior staphylomas in myopic eyes with axial length shorter than 26.5 millimeters. American Journal of Ophthalmology 2016; 162: 180-190.e1. https://doi.org/10.1016/j.ajo.2015.11.016
9. Liu HH, Xu L, Wang YX, Wang S, You QS, Jonas JB. Prevalence and progression of myopic retinopathy in Chinese adults: The Beijing eye study. Ophthalmology 2010; 117 (9): 1763-1768. https://doi.org/10.1016/j.ophtha.2010.01.020
10. Ctori I, Huntjens B. Repeatability of foveal measurements using Spectralis optical coherence tomography segmentation software. PLoS One 2015; 10 (6): e0129005. https://doi.org/10.1371/journal.pone.0129005
11. Kim JH, Lee SH, Han JY, Kang HG, Byeon SH et al. Comparison of individual retinal layer thicknesses between highly myopic eyes and normal control eyes using retinal layer segmentation analysis. Scientific Reports 2019; 9 (1): 14000. https://doi.org/10.1038/s41598-019-50306-w
12. Ye J, Wang M, Shen M, Huang S, Xue A et al. Deep retinal capillary plexus decreasing correlated with the outer retinal layer alteration and visual acuity impairment in pathological myopia. Investigative Ophthalmology & Visual Science 2020; 61 (4): 45. https://doi.org/10.1167/iovs.61.4.45
13. Liu X, Shen M, Yuan Y, Huang S, Zhu D et al. Macular thickness profiles of intraretinal layers in myopia evaluated by ultrahigh-resolution optical coherence tomography. American Journal of Ophthalmology 2015; 160 (1): 53-61.e2. https://doi.org/10.1016/j.ajo.2015.03.012
14. Campbell JP, Zhang M, Hwang TS, Bailey ST, Wilson DJ et al. Detailed vascular anatomy of the human retina by projection-resolved optical coherence tomography angiography. Scientific Reports 2017; 7: 42201. https://doi.org/10.1038/srep42201
15. Ohno-Matsui K, Kawasaki R, Jonas JB, Cheung CM, Saw SM et al. META-analysis for pathologic myopia (META-PM) study group. International photographic classification and grading system for myopic maculopathy. American Journal of Ophthalmology 2015; 159 (5): 877-883.e7. https://doi.org/10.1016/j.ajo.2015.01.022
16. Lutty GA, McLeod DS. Development of the hyaloid, choroidal and retinal vasculatures in the fetal human eye. Progress in Retinal and Eye Research 2018; 62: 58-76. https://doi.org/10.1016/j.preteyeres.2017.10.001
17. Yildirim Y, Kaya A, Kar T. Temperature control role of the choroid may affect choroidal thickness after dynamic exercise. Indian Journal of Ophthalmology 2015; 63 (12): 930. https://doi.org/10.4103/0301-4738.176033
18. Ivanova E, Toychiev AH, Yee CW, Sagdullaev BT. Intersublaminar vascular plexus: the correlation of retinal blood vessels with functional sublaminae of the inner plexiform layer. Investigative Ophthalmology & Visual Science 2014; 55 (1): 78-86. https://doi.org/10.1167/iovs.13-13196
19. Hasegawa T, Okamoto M, Masuda N, Ueda T, Ogata N. Relationship between foveal microstructures and visual outcomes in eyes with resolved central serous chorioretinopathy. Graefe's Archive for Clinical and Experimental Ophthalmology 2015; 253 (3): 343-350. https://doi.org/10.1007/s00417-014-2695-2

20. Ersoz MG, Karacorlu M, Arf S, Hocaoglu M, Sayman Muslubas I. Outer nuclear layer thinning in pachychoroid pigment epitheliopathy. Retina 2018; 38 (5): 957-961. https://doi.org/10.1097/IAE.0000000000001655

21. Jonas JB, Xu L. Histological changes of high axial myopia. Eye 2014; 28 (2): 113-117. https://doi.org/10.1038/eye.2013.223

22. Teberik K, Kaya M. Retinal and choroidal thickness in patients with high myopia without maculopathy. Pakistan Journal of Medical Sciences 2017; 33 (6): 1438-1443. https://doi.org/10.12669/pjms.336.13726

23. Abbott CJ, Grünert U, Pianta MJ, McBrien NA. Retinal thinning in tree shrews with induced high myopia: optical coherence tomography and histological assessment. Vision Research 2011; 51 (3): 376-385. https://doi.org/10.1016/j.visres.2010.12.005

24. Lam DS, Leung KS, Mohamed S, Chan WM, Palanivelu MS et al. Regional variations in the relationship between macular thickness measurements and myopia. Investigative Ophthalmology & Visual Science 2007; 48 (1): 376-382. https://doi.org/10.1167/iovs.06-0426

25. Sato A, Fukui E, Ohta K. Retinal thickness of myopic eyes determined by Spectralis optical coherence tomography. British Journal of Ophthalmology 2010; 94 (12): 1624-1628. https://doi.org/10.1136/bjo.2009.165472

26. Ng DS, Cheung CY, Luk FO, Mohamed S, Brelen ME et al. Advances of optical coherence tomography in myopia and pathologic myopia. Eye 2016; 30 (7): 901-916. https://doi.org/10.1038/eye.2016.47

27. Huynh SC, Wang XY, Rochtchina E, Mitchell P. Distribution of macular thickness by optical coherence tomography: Findings from a population-based study of 6-year-old children. Investigative Ophthalmology & Visual Science 2006; 47 (6): 2351-2357. https://doi.org/10.1167/iovs.05-1396

28. Li M, Yang Y, Jiang H, Gregori G, Roisman L et al. Retinal microvascular network and microcirculation assessments in high myopia. American Journal of Ophthalmology 2017; 174: 56-67. https://doi.org/10.1016/j.ajo.2016.10.018

29. Mo J, Duan AL, Chan SY, Wang XF, Wei WB. Application of optical coherence tomography angiography in assessment of posterior scleral reinforcement for pathologic myopia. International Journal of Ophthalmology 2016; 9 (12): 1761-1765. https://doi.org/10.18240/ijo.2016.12.10

30. Wang T, Li H, Zhang R, Yu Y, Xiao X et al. Evaluation of retinal vascular density and related factors in youth myopia without maculopathy using OCTA. Scientific Reports 2021; 11 (1): 15361. https://doi.org/10.1038/s41598-021-94909-8

31. Ye J, Lin J, Shen M, Chen W, Zhang R et al. Reduced radial peripapillary capillary in pathological myopia is correlated with visual acuity. Frontiers in Neuroscience 2022; 16: 818530. https://doi.org/10.3389/fnins.2022.818530